

Cauchy - Rayleigh CFAR for Ship Detection in Synthetic Aperture Radar

Odysseas PAPPAS, David BULL, Alin ACHIM

Visual Information Laboratory
University of Bristol, BS8 1UB, Bristol, UK

`o.pappas@bristol.ac.uk, dave.bull@bristol.ac.uk alin.achim@bristol.ac.uk`

Résumé – Le radar à synthèse d’ouverture (RSO) est actuellement l’une des modalités de télédétection les plus prometteuses pour la surveillance à grande échelle des océans et de l’activité maritime. Étant donné la diversité des applications en imagerie RSO, une riche littérature existe sur la modélisation statistique des images issues de cette modalité. Des travaux récents montrent notamment la capacité des lois de probabilité à queue lourde à correctement modéliser ces données, à travers par exemple des distributions telles que les alpha-stables ou la distribution de Rayleigh généralisée. Certaines applications comme la détection de navires en mer n’ont cependant pas encore bénéficié de l’utilisation de ces modèles statistiques récemment proposés. Dans cet article, nous proposons un détecteur par taux de fausse alarme constant (TFAC) basé sur une modélisation Cauchy-Rayleigh et son application à la détection de navires en mer. Nous montrons à l’aide de données haute résolution issues de TerraSAR-X que l’approche proposée donne de meilleurs résultats que des algorithmes existants, parmi lesquels le TFAC combiné à une loi de Weibull.

Abstract – Synthetic Aperture Radar (SAR) has over the years evolved to be one of the most promising remote sensing modalities for large-scale monitoring of the ocean and maritime activity. The use of SAR imagery in a variety of monitoring applications has motivated significant research on the statistical modelling of such images, with recent work focusing on the ability of the data’s heavy-tailed nature to be accurately modelled using distributions such as the α -stable and the Generalised Rayleigh distribution. Certain SAR applications, such as the detection of ships at sea have however as of yet not benefited from the use of these newly proposed statistical models. In this paper we present a Cauchy-Rayleigh Constant False Alarm Rate (CFAR) detector for the detection of ships at sea, showing that it can achieve superior performance to other previously used variants such as Weibull CFAR. We demonstrate the performance of our detector on high resolution TerraSAR-X data.

1 Introduction

Synthetic Aperture Radar has proven in the past years to be an excellent remote sensing modality for a plethora of monitoring tasks, largely due to its ability to operate at all times and regardless of weather and cloud coverage, giving it a clear advantage over optical and infrared sensors [1]. Some of these applications include mapping, agricultural monitoring, search and rescue applications and of course the monitoring of maritime activity, a key part of which is the detection of ships at sea.

This can be a rather complicated task as ships tend to appear as extremely small targets within high-resolution SAR images, providing little shape information to work with. In terms of intensity, ships typically appear as bright targets as the radar cross section (RCS) of a ship is much higher than that of sea clutter due to the large number of radar wave bounces caused by the ship’s metal superstructure (compared to the sea surface) [3]. Modern SAR platforms can produce high-resolution images where the sea wake caused by the ship, as well as waves due to wind and other clutter can become visible over the sea surface. This results in a more heterogeneous background, against which the detection of a ship target becomes more challenging.

This known target profile of high intensity compared to the background is strong motivation towards a threshold-based detection method. Most approaches proposed in the literature revolve around the use of a Constant False Alarm Rate (CFAR) detector and variants thereof. The standard cell-averaging CFAR detector estimates the level of noise around a pixel of interest by calculating the average power level in a neighbourhood around the pixel, while exempting those in a band directly around it (guard cells).

As with any imaging modality, accurate statistical modelling of the data is of paramount importance to effective processing and interpretation. In the case of SAR imagery, the otherwise typical assumption of a Gaussian distribution for the background does not hold; instead, distributions more suitable to capturing the heavy-tailed nature of the data must be employed. Examples of such heavy-tailed distributions that have been employed for SAR modelling in the past include the Log-normal distribution, Weibull [4] [5] and K -distribution [9].

While these more heavy-tailed distributions are a step in the right direction, they are still not capable of accurately modelling the histograms of modern SAR images - they often fail to account for extremely heavy tails or highly skewed data. Figure 1 for example demonstrates how the tails of the histogram data

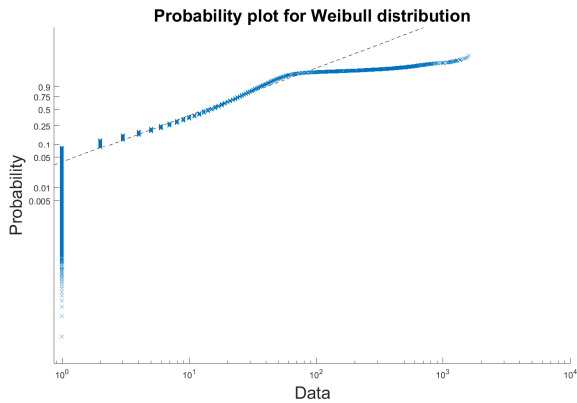


FIGURE 1 – Comparative probability plot of TerraSAR-X histogram versus a Weibull fit, showing the inability of the model to accurately account both for extremely low or high values.

for a TerraSAR-X image deviate significantly from the dotted line representing a Weibull fit.

This crucial problem of statistical modelling is therefore not closed, with ever more accurate models being constantly proposed in the literature. This is in part a consequence of the changing nature of the data itself. As the spatial resolution of SAR instruments increases, the associated reduction of scatterers per resolution cell leads to an increase of the appreciability of backscattering responses from distinct ground features, meaning SAR images with complex land/sea topologies now exhibit ever more so heavy-tailed and/or bimodal histograms [6].

Recent efforts in this direction include the use of the α -stable distribution for SAR modelling [8], the Generalised Gamma Distribution and the Generalised Gamma Mixture Model [7] [6] and the Generalised, Heavy-Tailed Rayleigh Model [2], [1]. However, many of these proposed distributions have not yet been applied to more practical SAR processing problems, in part due to their complicated nature, often lacking analytical, closed-form expressions and difficulties regarding parameter estimation.

In this paper we investigate the use of the Heavy-Tailed Rayleigh Model, and in particular the special case of the Cauchy-Rayleigh, in the context of a CFAR detector. We demonstrate how an analytical, closed-form expression for the CFAR threshold can be derived from the Cauchy-Rayleigh pdf and its promising performance for the detection of ships at sea in SAR images.

The paper is organised as follows : Section 2 briefly introduces the Generalised Rayleigh model and its specific cases like the Cauchy-Rayleigh distribution. The Cauchy-Rayleigh CFAR detector is described in Section 3. Section 4 presents results of the detector on TerraSAR-X data, followed by a relative discussion and conclusions.

2 The Generalised, Heavy-Tailed Rayleigh Model

SAR image formation theory was initially centred on the assumption that the real and imaginary parts of the received radar return signals are Gaussian distributed, resulting in a Rayleigh model for the SAR amplitude image. This assumption has recently been challenged and replaced by an assumption of “alpha-stability” for the radar returns [2].

The $S\alpha S$ distribution has garnered significant attention as a statistical model in recent years, partly due to its desirable stability property (linear combinations of jointly stable variables are also stable) and the fact that according to the generalised central limit theorem the sum of a large number of i.i.d. processes approaches the α -stable law [10].

Under this assumption of jointly $S\alpha S$ real and imaginary parts of the received signal, Kuruoglu and Zerubia [2] derive the *Heavy-Tailed Rayleigh* distribution, the pdf for amplitude SAR images of which is given below :

$$p_A(x) = x \int_0^\infty u \exp(-\gamma u^\alpha) J_0(ux) du \quad (1)$$

where α is the characteristic exponent ($0 < \alpha \leq 2$), γ is the dispersion of the distribution ($\gamma > 0$) and J_0 is a zero order Bessel function of the first kind. As the name implies, this distribution has significantly thicker tails than the typical Rayleigh distribution and is better suited to describing impulsive data.

Special cases of the Heavy-tailed Rayleigh model include the case of $\alpha = 2$, for which the pdf reduces to the classical Rayleigh distribution (2) (similar to how the $S\alpha S$ distribution reduces to Gaussian for $\alpha = 2$),

$$p_A(x) = \frac{x}{2\gamma} \exp\left(-\frac{x^2}{4\gamma}\right) \quad (2)$$

while for $\alpha = 1$ the pdf reduces to the following form which the authors refer to as Cauchy - Rayleigh model

$$p_A(x) = \frac{x\gamma}{(x^2 + \gamma^2)^{3/2}} \quad (3)$$

It should be noted here that the pdf of (1) refers to an amplitude image, and this is the case that will be used for the remainder of this paper. Adapting the pdf and all following derivations for the case of an intensity image is straight-forward by recalling the following relationship (4).

$$p_A(x) = 2xp_I(x^2) \quad (4)$$

2.1 Parameter Estimation

Being able to accurately estimate the parameters of any statistical model is paramount to it having any practical use. We opt here to use the parameter estimation method proposed in [1], based on the use of the Mellin transform & log-cumulants as proposed by Nicolas [12] while taking into account the presence of multiplicative, Nakagami distributed speckle noise often present in SAR data.

The entire derivation is quite lengthy and can be found in full in [1], we recap here that α and γ are given by the following respective equations :

$$\hat{\alpha} = \sqrt{\frac{\psi(1, 1)}{\hat{k}_{(2)} - \frac{1}{4}\psi(1, L)}} \quad (5)$$

$$\hat{\gamma} = \left[\frac{\exp\left(\hat{k}_{(1)} + \psi(1)\frac{1-\alpha}{\alpha} - \frac{1}{2}(\psi(L) - \log(L))\right)}{2} \right]^\alpha \quad (6)$$

where ψ is the Digamma function and $\psi(r, \cdot)$ is the r_{th} derivative of the Digamma function (also known as the Polygamma function), $\hat{k}_{(1)}, \hat{k}_{(2)}$ are the first- and second-order second-kind cumulants as defined using the Mellin transform [12] and L is the number of looks in the SAR image [1].

3 Cauchy-Rayleigh CFAR

Constant False Alarm Rate detectors aim to detect bright targets of interest by thresholding against their background; an adaptive threshold is used for each pixel so that a desired probability of false alarm (P_{FA}) is maintained over the entire image. This threshold is derived using a sliding window centred on the pixel of interest while at the same time excluding immediately surrounding pixels (guard band) as it is assumed they may also be part of a potential target.

Assuming a distribution model $f_{pdf}(x)$ for the background, the P_{FA} for a given threshold T is given by :

$$P_{FA} = 1 - \int_{-\infty}^T f_{pdf}(x) dx = \int_T^{\infty} f_{pdf}(x) dx \quad (7)$$

Having settled on a statistical model and the acceptable P_{FA} for a particular application, an analytical expression for the threshold T can then typically be derived from (7).

This direct approach may not always be feasible - in the case of the Generalised Rayleigh model, the integral in (1) cannot be analytically evaluated except for the specific values of α that correspond to (2) and (3) [2]. Numerical evaluation of (1) is possible and can perhaps be used to compile look-up tables of appropriate thresholds for varying values of P_{FA} ; an approach that has been employed in the past for distributions like the α -stable, which lacks a closed-form pdf [8].

We instead opt here to limit our model to the particular case of the Cauchy-Rayleigh (3) and to obtain an analytic, closed-form expression for the threshold T . We consider this approach to be beneficial compared to prior attempts for a number of reasons. Firstly, it has been shown that the special case of Cauchy-Rayleigh alone is capable of modelling the pdf of high resolution SAR images to a better degree than previously used distributions like the Weibull and K -distributions [2] [1] [8]. Secondly, the existence of a closed-form solution allows for the calculation of the exact desired T value instead of the closest fit available in the look-up table. Finally, eliminating the need

to estimate α (as it is assumed $\alpha = 1$) lends more robustness to the detector, as only an estimate for γ (6) is now required.

By plugging (3) in (7) we can obtain

$$P_{FA} = \int_T^{\infty} \frac{x\gamma}{(x^2 + \gamma^2)^{3/2}} dx = \frac{\gamma}{\sqrt{\gamma^2 + T^2}} \quad (8)$$

and thus the threshold can be calculated by

$$T = \sqrt{\frac{\hat{\gamma}^2}{P_{FA}^2} - \hat{\gamma}^2} \quad (9)$$

4 Results

We present results of our algorithm on SAR images from the TerraSAR-X platform (©DLR e.V. 2013, Distribution AIRBUS DS Geo GmbH). The instrument is an X-band Synthetic Aperture Radar operating in ScanSAR (SC) mode, in HV polarisation and it is imaging part of the Panama Canal.

As there is no ground truth available for the visible sea traffic, it has been evaluated visually using direct ship radar return signatures as well as transverse and turbulent ship wake where present, in accordance with the information and guidelines provided in the SAR Marine User's Manual [11]. The P_{FA} of the CFAR detector has been set to 0.01 for all experiments.

Region 1, shown in Figure 2, contains 11 discernible ship targets with part of a pier structure also visible in the lower right. The Weibull CFAR detector produces a high number of false positives over the sea surface, to the effect where the masked output looks similar to the original image. The Cauchy-Rayleigh CFAR on the other hand is capable of separating the RCS of the ship targets from the sea background and even the pier structure, producing virtually no false positives while maintaining detection of all 11 discernible vessels. This largely due to the distribution's ability to not only model more accurately the heavier tails but also the large number of low-level values.

Figure 3 shows a similar scenario, this time with 8 ship targets and a small islet barely visible on the bottom of the image. The comparison this time is against a standard Rayleigh CFAR which, similar to the Weibull also produces a larger number of false positives over the sea surface.

5 Conclusions

In this paper we have commented on the state of the art on SAR image modelling and the discrepancy between the models proposed in the literature and the models actually utilised for CFAR-based ship detection. We have therefore demonstrated the use of the Cauchy-Rayleigh CFAR detector for ship detection in TerraSAR-X images, showing improved performance compared to other classic models like the Weibull distribution.

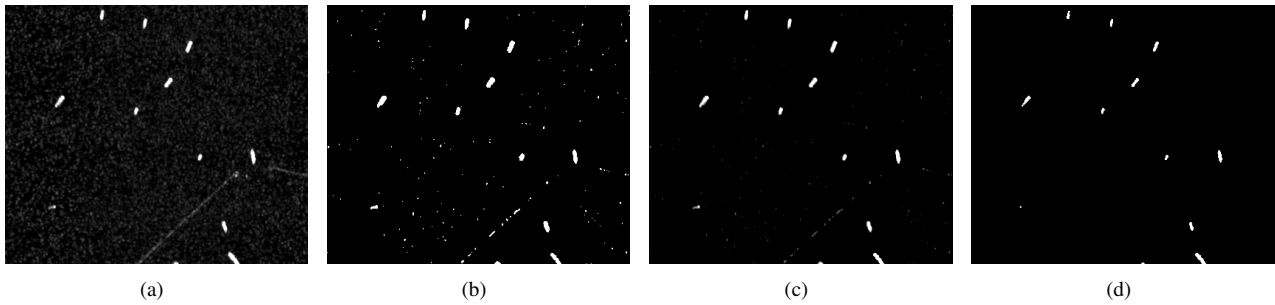


FIGURE 2 – (a) TerraSAR-X Region 1, (b) Weibull CFAR detections, (c) Weibull CFAR mask over original image and (d) proposed Cauchy-Rayleigh CFAR.

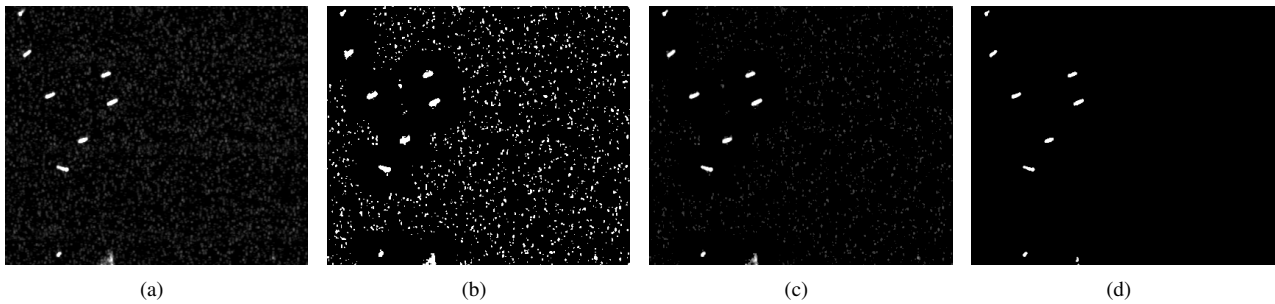


FIGURE 3 – (a) TerraSAR-X Region 2, (b) Rayleigh CFAR detections, (c) Rayleigh CFAR mask over original image and (d) proposed Cauchy-Rayleigh CFAR.

Références

- [1] A. Achim, E. E. Kuruoglu et J. Zerubia. *SAR Image Filtering Based on the Heavy-Tailed Rayleigh Model*. IEEE Transactions on Image Processing, 15, pp. 2686-2693, 2006.
- [2] E. E. Kuruoglu et J. Zerubia. *Modeling SAR Images With a Generalization of the Rayleigh Distribution*. IEEE Transactions on Image Processing, 13, pp. 527-533, 2004.
- [3] J. Ai, X. Qi, W. Yu, Y. Deng, F. Liu et L. Shi. *A New CFAR Ship Detection Algorithm Based on 2-D Joint Log-Normal Distribution in SAR Images*. IEEE Geoscience and Remote Sensing Letters, 7, pp. 806-810, 2010.
- [4] O. Pappas, A. Achim et D. Bull. *Superpixel-guided CFAR Detection of Ships at Sea in SAR Imagery*. IEEE International Conference on Acoustics, Speech and Signal Processing (ICASSP), pp. 1647-1651, New Orleans, 2017.
- [5] A. Poumottaghi et S. Gazor. *A CFAR Detector in a Non-homogeneous Weibull Clutter*. IEEE Transactions on Aerospace and Electronics Systems, 48, pp. 1747-1758, 2012.
- [6] H. Li, V. A. Krylov, P. Fan, J. Zerubia et W. J. Emery. *Unsupervised Learning of Generalized Gamma Mixture Model with Application in Statistical Modeling of High-Resolution SAR Images*. IEEE Transactions on Geoscience and Remote Sensing, 54, pp. 2153-2170, 2016.
- [7] H. Li, W. Hong, Y. Wu et P. Fan. *On the Empirical-Statistical Modeling of SAR Images With Generalized Gamma Distribution*. IEEE Journal of Selected Topics in Signal Processing, 5, pp. 386-397, 2011.
- [8] M. Liao, C. Wang, Y. Wang et L. Jiang. *Using SAR Images to Detect Ships From Sea Clutter*. IEEE Geoscience and Remote Sensing Letters, 5, pp. 194-198, 2008.
- [9] S. Kuttikkad et R. Chellappa. *Non-Gaussian CFAR Techniques for Target Detection in High Resolution SAR Images*. IEEE International Conference on Image Processing, pp. 910-914, 1994.
- [10] C. L. Nikias et M. Shao. *Signal Processing With Alpha-Stable Distributions and Applications*. New York, Wiley, 1995.
- [11] W. G. Pichel, P. Clemente-Colon, C. C. Wakerman et K. S. Friedman. *Ship and Wake Detection*. Synthetic Aperture Radar Marine User's Manual, Eds. C. R. Jackson et J. R. Apel, pp. 277-303, NOAA/NESDIS U.S. Department of Commerce, 2004.
- [12] J. M. Nicolas. *Introduction aux statistiques de deuxième espèce : applications des log-moments et des log-cumulants à l'analyse des lois d'images radar*. Traitement du Signal, 19, pp. 139-167, 2002.